Polym. Bull. (2011) 66:1231–1253
DOI 10.1007/s00289-010-0395-6

ORIGINAL PAPER

Nanostructure morphology and dynamic rheological properties of nanocomposites based on thermoplastic polyurethane and organically modified montmorillonite

A. K. Barick · D. K. Tripathy

Received: 22 March 2010 / Revised: 2 July 2010 / Accepted: 28 September 2010 /
Published online: 2 November 2010

Abstract Thermoplastic polyurethane (TPU) nanocomposites based on organophilic-layered silicates were prepared via melt blending. Wide angle X-ray diffraction (WAXD) and transmission electron microscope (TEM) were employed to investigate the state and mechanism of exfoliation of the layered silicate within TPU matrix. The TPU nanocomposites were found to have a partially exfoliated morphology at lower clay loading, whereas the morphology changed to an intercalated nanostructure at higher clay loadings. The effect of the state of dispersion of organoclay on rheological properties of the nanocomposites were carried out by rubber process analyzer (RPA), which exhibited more pronounced shear thinning behavior, and increased storage and loss modulus with the increase in organoclay content. The pseudo-plastic like behavior was observed due to change in liquid-like to solid-like behavior of nanoclay-filled systems.

Keywords Thermoplastic polyurethane · Organoclay · Nanocomposites · Melt intercalation Morphology · Rheological properties

Introduction

In recent years, polymer/layered silicate nanocomposites have drawn a lot of attention because of their academic and industrial importance. Polymer–clay nanocomposites can dramatically improve the mechanical reinforcement [1], high temperature durability [2], provide enhanced barrier property [3], and reduce flammability [4] as compared to standard conventional macro- and micro-fillers,

A. K. Barick · D. K. Tripathy (✉)
Rubber Technology Centre, Indian Institute of Technology, Kharagpur 721302, West Bengal, India
e-mail: dkt@rtc.iitkgp.ernet.in

A. K. Barick
e-mail: akbarick@gmail.com

which makes it commercially viable. Lightweight and economic competitiveness using a minimal amount of reinforcing materials are other advantages of polymer–clay nanocomposites that lead to enhancement of various material properties, which make them suitable for a variety of applications, such as automotive, electronic, food packaging, biotechnology, biomedical, tissue engineering, etc.

Among different methods used for preparing polymer nanocomposites the melt intercalation method is the most industrially viable technique for preparation of polymer–clay nanocomposites due to it's technically soundness, versatility, environmentally benign characteristics, and good compatibility with the conventional polymer processing techniques. Since the possibility of direct melt intercalation was first demonstrated by Viaia and Giannelis [5], it has become a primary process for the preparation of intercalated/exfoliated polymer nanocomposites without in situ intercalative polymerization and/or solution intercalation technique. The preparation of polyurethane nanocomposites based on organosilicate through melt compounding technique was first reported by Finnigan et al., who achieved a large increase in stiffness, higher hysteresis, and permanent set while tensile strength and elongation were not substantially improved on addition of organosilicate. This result also illustrates that the organosilicates are dispersed and delaminated effectively in the segmented polyurethane matrix via melt processing route where molecular diffusion and shear stress plays a good driving force for intercalation between the polymer and nanofillers [1]. Very little work has been carried out on nanoclay-based TPU nanocomposites (TPUCN) prepared by melt intercalation technique in spite of the obvious advantages of this approach [6–14].

The present study deals with the morphological and rheological characterization of TPU nanocomposites prepared by melt intercalation of TPU matrix phase into organically modified nanoclay (Cloisite 15A) dispersed phase. The main objective of the current work is the systematic investigation of the reinforcing effect of the organoclay dispersion on the dynamic rheological properties of the melt blended thermoplastic polyurethane–clay nanocomposites. Furthermore, the viscoelastic properties of the neat TPU and its organoclay nanocomposites were investigated over a broad strain, frequency, and temperature range.

Experimental

Materials

Polymer matrix

Commercial biomedical clear grade aliphatic, polyether-based thermoplastic polyurethane (Tecoflex® EG 80A injection grade) taken for this research work was procured from Lubrizol Advanced Materials, Thermedics™ Inc. Polymer Products, Ohio, USA. Tecoflex® EG 80A (around 35% of hard segments) having Shore A hardness = 72, specific gravity = 1.04 at 25 °C, and its constituent molecular formulation contains methylene bis(cyclohexyl) diisocyanate (HMDI) as hard

segment, polytetramethylene oxide (PTMO) as soft segment (molecular weight = 1000 g/mol), and 1,4 butane diol (BD) as chain extender.

Nanofiller

Commercial Cloisite 15A nanoclay used in this study was procured from the Southern Clay Products, Inc., Texas, USA. The Cloisite 15A is a layered organosilicate nanoclay based on a natural montmorillonite having density = 1.66 g/cm^3, d_{001} = 3.15 nm, cation exchange capacity (CEC) = 1.25 meq/g with dimethyl dehydrogenated tallow ammonium modifier (2M2HT) of tallow composition as ~65% C18; ~30% C16; ~5% C14.

Equipments

Mixing machine

TPU nanocomposites with different wt% of nanoclay loadings were prepared by batch processing method in a co-rotating internal batch mixer (Thermo Scientific HAAKE PolyLab OS Rheomix, Thermo Electron Corporation, Massachusetts, USA) having a mixing chamber volume of 85 cm^3. The compounds were passed once through a cold two roll mill (Farrel Bridge Limited, Lancashire, England) immediately after batch mixing to achieve about 2 mm thick sheets. The sample sheets were cut into small pieces and then pressed in a compression molding machine (Moore Press, Birmingham, UK).

Microstructural analysis

X-ray diffraction (XRD) analysis was performed with a high-resolution X-ray diffractometer (X'Pert PRO, Philips PANalytical B.V., Almelo, Netherlands) with Cu Kα (λ = 0.15418 nm) radiation source operated at voltage of 40 kV and 30 mA electric current. The samples were scanned from 1 to 10° (2θ) at a scan rate of 2°/min and samples were placed vertically in front of the X-ray source.

The microstructural analysis of nanocomposites were carried out using a high-resolution transmission electron microscope (JEM 2100, JEOL Limited, Tokyo, Japan) attached with charge couple device (CCD) camera (Gatan, Inc., California, USA). The specifications for TEM are as follow; point to point resolution = 0.194 nm, lattice resolution = 0.14 nm, tilt angle = 24°, acceleration voltage = 200 keV, and electron gun of lanthanum hexaboride (LaB_6) filament type. The samples for TEM analysis were prepared using cryo-ultramicrotome (Ultracut UCT, Leica Mikrosystems GmbH, Vienna, Austria) with Leica EM FCS low temperature sectioning system. Freshly sharpened diamond knives with cutting edges of 45° were used to obtain cryosections of 50–70 nm thickness specimens at ambient temperature of −70 to −80 °C.

Rheological measurement

The viscoelastic properties of the samples were found out using rubber process analyzer (RPA 2000, Alpha Technologies, Ohio, USA). The dynamic frequency

sweep test was carried out at a strain of 0.98% and temperature of 145 °C with a frequency range of 0.033–30.833 Hz. The temperature sweep test was carried out in shear mode at a constant angular frequency of 16.667 Hz and shear strain of 2.79% in the temperature range of 40–225 °C. The dynamic strain sweeps of the samples were studied at a frequency of 0.333 Hz and temperature of 145 °C with a strain range of 0.7–1256%. Stress relaxation experiment for the neat TPU and its nanocomposites were carried out using RPA at temperature of 60 °C and shear strain of 69.75% for a time period of 180 s.

Preparation of TPU/nanoclay nanocomposites

The internal batch mixer was used for melt blending of different compounds (1, 3, 5, 7, and 9 wt% of nanoclay in 100 wt% of polymer matrix) of thermoplastic polyurethane (TPU) and organically modified montmorillonite (OMMT) at 185 °C with a rotor speed of 100 rpm and mixing time of 6 min. Prior to mixing, nanoclay and TPU were dried in a vacuum oven at 80 °C for 12 h for evaporation of moisture content (if any in supplied materials). TPU and its nanocomposite sheet specimens with thickness of 2 mm are compression molded at 185 °C and 5 MPa pressure for 3 min. The molded sheets were cooled to room temperature through internal circulation of water under adequate pressure. The samples for mechanical testing were punched from the compression molded sheets. The virgin thermoplastic polyurethane sample is coded as "TPU" and TPU nanocomposite samples are designated as "TPUXA"; where "X" stands for wt% of organoclay in TPU matrix and "A" stands for Cloisite 15A organoclay.

Results and discussion

Dispersion of organoclays in TPU matrix

Wide angle X-ray diffraction (WAXD)

The XRD patterns of neat TPU, Cloisite 15A, and TPU nanocomposites containing various fractions of nanoclay are shown in Fig. 1. The XRD pattern of the Cloisite 15A organoclay shows two characteristic peaks at $d_{001} = 3.457$ nm and $d_{002} = 1.25$ nm with 2θ values 2.555° and 7.085°, respectively. After melt intercalation, the intensity of the diffraction peaks corresponding to the organoclay are considerably reduced and get broaden while new peaks at $d_{001} = 3.72$ nm and $d_{002} = 1.935$ nm appear with $2\theta = 2.375°$ and 4.565°, respectively, corresponding to the non-exfoliated TPU nanocomposites. The shifting of diffraction peaks to lower angle suggested an increase in interlayer spacing or gallery of the clay silicate layers, which is referred to an intercalated nanostructure. However, the intensity of characteristic diffraction peak of the TPU nanocomposites ($2\theta = 4.565°$ and 2.375°) reduces and get broaden when the clay content of the nanocomposites were lower than 5 wt%. The disappearance of the clay interlayer diffraction peaks indicate exfoliation of the clay platelets into nanoscale layers and broadening of the

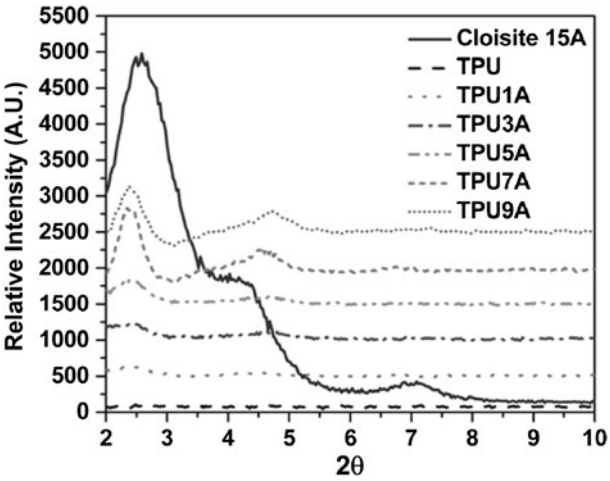

Fig. 1 WAXD lower angular patterns of neat Cloisite 15A nanoclay, pristine TPU, and its nanocomposites with 1, 3, 5, 7, and 9 wt% of Cloisite 15A nanoclay loadings

peak is considered to be the result of partial exfoliation of randomly dispersed silicate layers in the TPU matrix through the melt mixing process. This is clearly evident from the TEM micrographs shown in the Fig. 2. Table 1 shows the degree of dispersion of nanoclay platelets in TPU matrix that evaluated through estimation of the distance between individual platelets using "Bragg's law" after mixing with TPU matrix.

Transmission electron microscope (TEM)

Figure 2 shows the TEM microphotographs of TPU/organoclay nanocomposites with different amount of nanoclay. At lower clay content (1 and 3 wt%), most of the nanoclay platelets are uniformly dispersed in the TPU matrix but the aggregation of clay platelets increases with increase in nanoclay content ($\leq$5 wt%), which further confirmed the X-ray diffraction results. Furthermore, the TEM microphotographs clearly show that the most of the clay layers are parallel to the surface of the films and are homogeneously dispersed throughout the polymer matrix. The appearance of some clusters or agglomerated clay particles are possibly due to the higher loading of nanoclay into TPU matrix. In addition, small clusters of intercalated silicates and a portion of exfoliated silicates are also visible in all images. It appears that significantly mixed morphology, i.e., regions of both partially exfoliated and intercalated nanostructures were achieved via melt compounding. This result can be attributed to the higher shear stresses associated with the melt processing, which promote the fracturing and separation of layered silicate stack into individual clay units. The organically modified montmorillonite (OMMT) with lower electrostatic force of interactions between clay layers facilitate enlargement of the interlayer gallery spacing and hence, the exfoliation and dispersion of individual silicate clay layers significantly increases in TPU matrix.

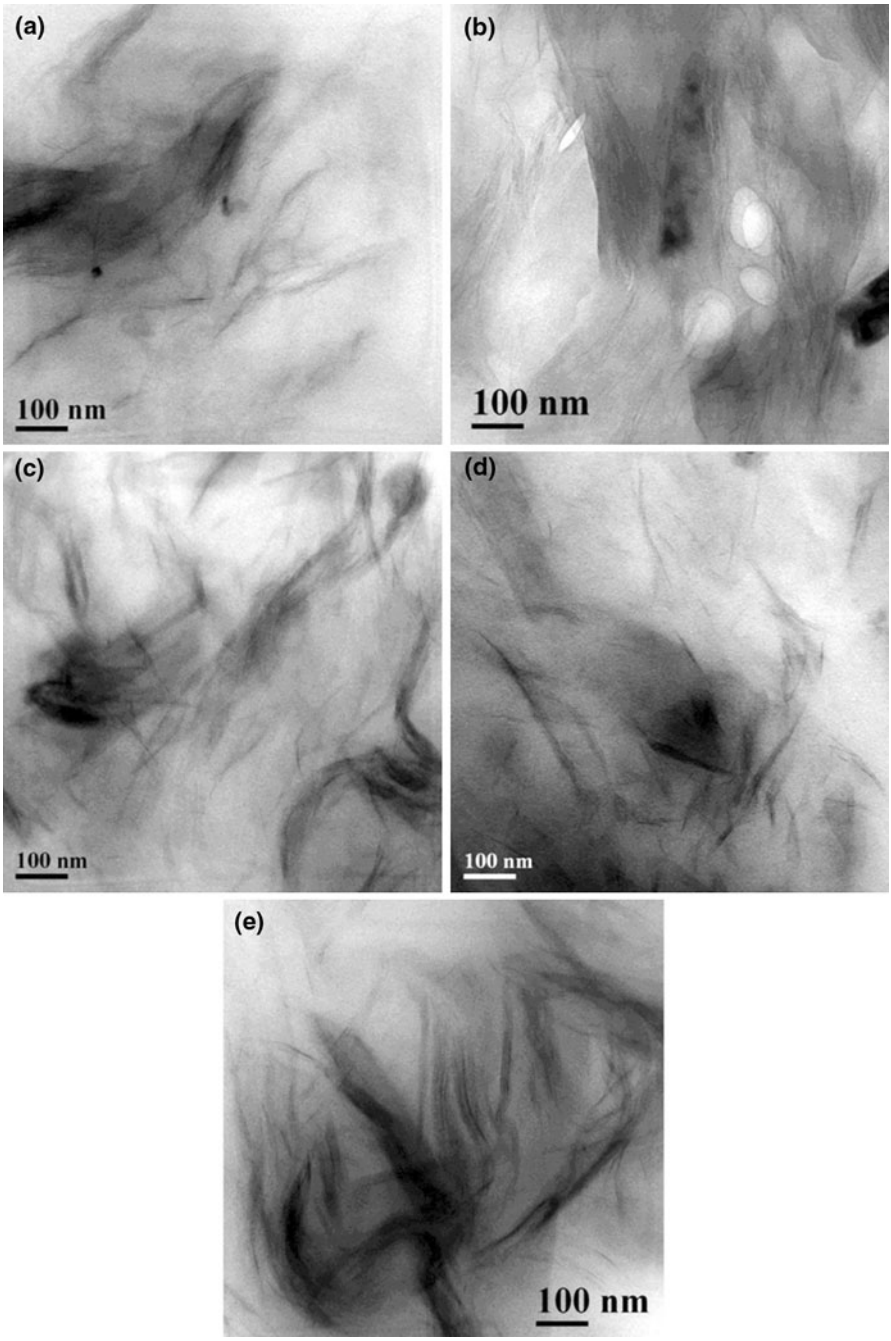

Fig. 2 Bright field TEM microphotographs of TPU nanocomposites with **a** 1 wt%, **b** 3 wt%, **c** 5 wt%, **d** 7 wt%, and **e** 9 wt% of Cloisite 15A nanoclay loadings at ×25,000 magnification

Table 1 Platelet spacing of the nanoclays and the nanocomposites

Sample codes	2θ (°)	Spacing between the platelets (nm)
Cloisite 15A	2.555	3.457 (d_{001})
	7.085	1.250 (d_{002})
TPU	No peak	Amorphous polymer
TPU1A	No peak	Fully exfoliated
TPU3A	No peak	Fully exfoliated
TPU5A	2.375	3.720 (d_{001}), partially exfoliated
	4.565	1.935 (d_{002}), intercalated
TPU7A	2.375	3.720 (d_{001}), partially exfoliated
	4.565	1.935 (d_{002}), intercalated
TPU9A	2.375	3.720 (d_{001}), partially exfoliated
	4.675	1.890 (d_{002}), intercalated

Dynamic rheological properties

Rubber process analyzer

Dynamic rheological behavior of polymer nanocomposites in molten state is very critical to understand and evaluate the processability and structure–property relationships for these materials. Furthermore, the melt rheology measurements can probe behavior of the relatively large material, which is crucial from the macroscopic point of view. Three vital criteria which are principal responsible for the significant implementation of the reinforcement mechanism in polymer nanocomposites are as follow: (i) the replacement of soft polymeric matrix component by more stiff and rigid nanofiller parts, (ii) the restriction imposed through incorporation of nanofiller particles on the random mobilization of polymer molecular chains on the nanofiller particle surfaces due to the filler–polymer interphase interaction, and (iii) The residual stress transfers from the flexible polymer matrix to the stable dispersed nanofillers through proper phenomena, provided that the nanofillers are having larger aspect ratio and highly active surface area. However, the interacting effects like formation of filler–filler aggregates, development of residual stresses, and/or internal defects accompanying with the polymer matrix or present at the interfacial region of matrix-filler makes the system more complicated for reliable prediction of the dynamic viscoelastic characteristic of the polymer–nanoclay nanocomposites.

Strain sweep test

The relationship of storage modulus (G') and loss modulus (G'') of TPU and its nanocomposites containing different wt% of OMMT loading with strain amplitude (γ) obtained by the dynamic strain sweep measurements are shown in Fig. 3a, b. The dynamic strain sweep test was applied in order to characterize the strain dependence of the viscoelastic properties and also to determine linear viscoelastic (LVE) region

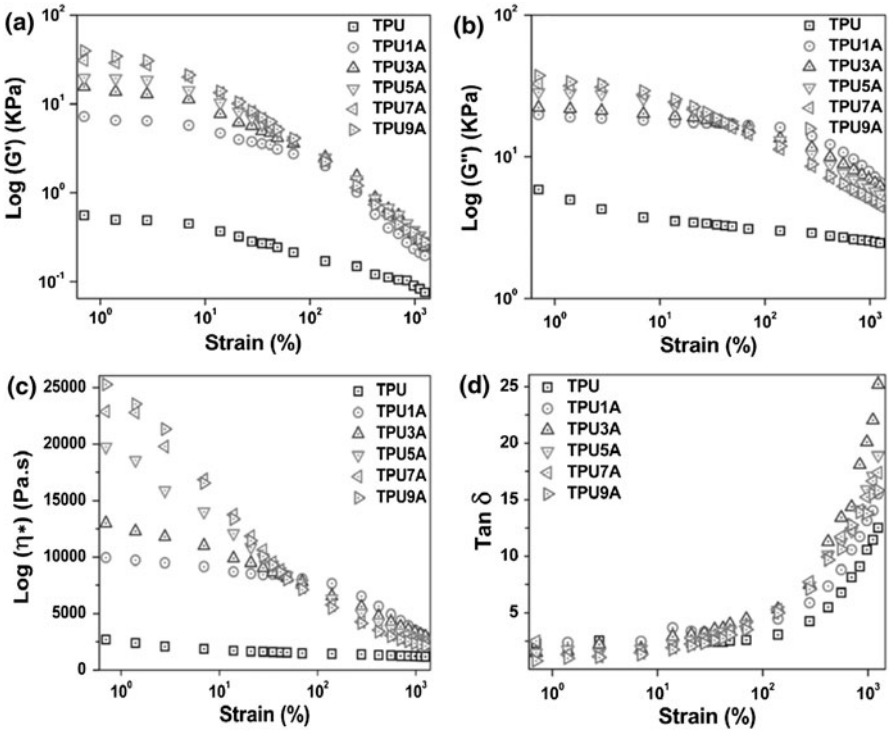

Fig. 3 Dynamic Strain sweep of **a** storage modulus (G'), **b** loss modulus (G''), **c** complex viscosity (η^*), and **d** damping factor (tan δ) for neat TPU and its nanocomposites containing various wt% of OMMT loadings at a test frequency of 0.333 Hz and at a temperature of 145 °C

of the TPU nanocomposite samples. The plateau region of the dynamic strain sweep experiment where the elastic modulus is independent of shear strain or oscillating stress is directly proportional to the applied angular strain, which is defined as the linear viscoelastic region of the nanocomposites. From Fig. 3a, b, it has been observed that the entire samples exhibit Newtonian plateau at low strain range but they show non-Newtonian plateau at high strain amplitudes. It has been observed that the region of linear viscoelastic behavior is changed greatly in the presence of the intercalated layered silicates. The Newtonian plateau is rapidly diminished with increase in nanoclay concentration, which indicates that the TPU nanocomposites show non-linear viscoelastic behavior at lower strain rate. It was observed that the low strain plateau modulus readily increases with increase in organoclay content. The transition point at the deviation region from the linear to non-linear viscoelastic behavior is defined as critical strain (γ_c) value, which substantially varies with the wt% of nanoclay content and nanostructure dispersion morphology of the nanocomposites. The non-linearity in the viscoelastic response of nanocomposites arise at higher strain is mainly attributed to the partial breakdown of highly entangled network structure present within the matrix system. TPU nanocomposite reinforced with 9 wt% nanoclay exhibits a non-linear viscoelastic behavior when shear strain

amplitude is as low as 1% as a result the following dynamic frequency scan measurements were carried out at $\gamma_0 = 0.98\%$. It is found that γ_c is inversely related to the volume fraction of the layered silicates (ϕ_e), which indicates that the strain limit of linear viscoelastic region of TPU nanocomposites are very sensitive to the concentration of layered silicates at molten state and decreases logarithmically with the addition of clay even at a low clay loading of 1 wt%. The γ_c value for the pristine TPU matrix is about 100%, which decreases to a strain level of less than 10% for the high organoclay loaded nanocomposites. It is concluded that the presence of nanometer-scale dispersed clay particles and individual silicate layers is very sensitive to small strain amplitude as a result of which the critical strain amplitude deduced from both G' and G'' dramatically decreases with wt% of nanoclay content. This result also indicates that the yield point of the modulus–strain curve is shifted to lower strain that makes the system more rigid and brittle. The dramatic reduction of modulus value with increase in the strain amplitude for all the clay reinforced compounds may be explained by the "Payne effect" [15]. The comparison between value of G' with that of G'' of the neat TPU and TPU nanocomposites show that the G'' is greater than G' ($\tan \delta > 1$). It reveals that with increase in OMMT content, the viscous behavior of the TPU dominates over the elastic behavior at all the level of filler loading. After a certain strain amplitude (around 40%), the rate of decrease in the loss modulus (G'') is more pronounced in case of the highly nanoclay-filled systems due to the disruption of the continuous three dimensional network structure of the fillers that interpenetrate into the TPU matrix. The network structure of the sample emanates from the presence of entanglements of amorphous soft segment and ordered crystalline hard segment domain of TPU matrix. The network structure of the unfilled matrix sustains large deformation while formation of a new nanostructure occurs in nanoclay-filled TPU matrix. Furthermore, layered silicate filler decreases the entanglement density of amorphous zone making the network structure weak, which does not resist large deformation at higher strain region as compared to the pristine counterpart.

Figure 3c shows the plot of the variation of complex viscosity (η^*) with dynamic strain at a particular applied frequency. At low strain, the η^* value of the pure TPU and TPU nanocomposites are not changed or slightly reduced with strain, which corresponds to the linear viscoelastic behavior of materials. The η^* of samples decrease with increase in strain, but the rate of decrease is more pronounced after 10% strain in case of nanoclay-filled TPU due to the strong shear thinning behavior. At around 49% shear strain, the η^* of all the TPU nanocomposites converged towards a single point, which may be resulted from the directional orientation of polymer chains and silicate layers along the flow direction. Also retention of the η^* at high strain is due to the strain-induced crystallization of TPU chains in the presence of organoclay that act as a nucleating agent.

The effect of strain on the damping behavior of neat TPU and its nanocomposites are shown in Fig. 3d. Tan δ is found to increase with shear strain due to the disruption of the filler networks and molecular chain slippage. The strong interfacial interaction may definitely impede the chain mobility during the rheological test that results the increase in loss angle. The energy losses under deformation condition of the nanoclay-filled system that resulted from internal frictions and

breaking/reforming of filler–polymer at contact points are the main cause of rise of tan δ with increase in strain. The enhancement of the tan δ is probably related to the strain hardening behavior of the samples once irreversible deformation occurs. At lower strain region (below 40%), the decrease in tan δ value with increase in the nanoclay concentration is possibly due to the reduction of the soft elastomeric phases imparted by rigid clay particles. This result also suggested that there is strong filler to matrix coupling. At higher strain region (above 40%), the tan δ value increases with increase in the nanoclay content because of the complete breakdown of the filler–filler network structures leading to development of the well-dispersed nanostructures, whereas at higher clay loading the tan δ value decreases due to the strong aggregation behavior of the nanoclay particles.

Frequency sweep test

The dynamic frequency sweep tests were carried out in the linear viscoelastic region ($\gamma = 0.98\%$) to study about the network formations and microstructural changes of the nanocomposites. The plot of log of G', G'', η^*, and loss tangent (tan δ) versus log of angular frequency resulting from the dynamic frequency scan measurements at 145 °C for neat TPU and TPU nanocomposites with various wt% of nanoclay loading are shown in Fig. 4a, b, c, and d, respectively. The low frequency region of rheological plot reflects the effect of nanostructure and state of dispersion of layered silicates on the viscoelastic properties of the nanocomposites. Furthermore, to find out the influence of nanoclay on the rheological behavior of the nanocomposites, the variation of modulus and η^* with the frequency (ω) were studied at low frequencies.

Figure 4a, b exhibits monotonically increase in G' and G'' with frequency at all wt% of nanoclay loading. The increase of G' and G'' are substantially higher in case of nanocomposites as compared to their pristine counterpart because of the strong filler–polymer interactions arising due to the clay–matrix tethering, uniform nanoscale dispersion, and larger surface area of clay particles exposed to the polymer chains [16]. The G' value increases monotonically with nanoclay loading at low frequency in contrast to that of pure TPU sample, which is mainly due to the contribution of intercalated nanoclays to G' of the TPU nanocomposites (G'_{nano}). The substantial enhancement of the low frequency G'_{nano} value as compared to the G' of the TPU matrix (G'_{matrix}) is mainly analyzed in terms of two effects: (a) the confinement effect (G'_{con}) and (b) the inter-particle interactions (G'_{inter}) [17]. At low frequency, the G' and G'' ranges are higher, which narrow down at high frequency. This is because at low frequency, there is enough time for unraveling of the entanglements leading to a large amount of relaxations, which results a lower value of both G' and G''. The slope of the curve particularly at lower frequency region noticeable decreases with increase in filler loading that refers to the rise in the elastic response of the TPU matrix. However, when a polymer sample is deformed at higher frequency the entanglement chains do not get sufficient relaxation time as a consequence the modulus becomes higher. At low frequency region, the neat TPU and TPU nanocomposite melts show liquid-like behavior ($G' < G''$) while substantially solid-like behaviors ($G' > G''$) at high frequency region. The transition

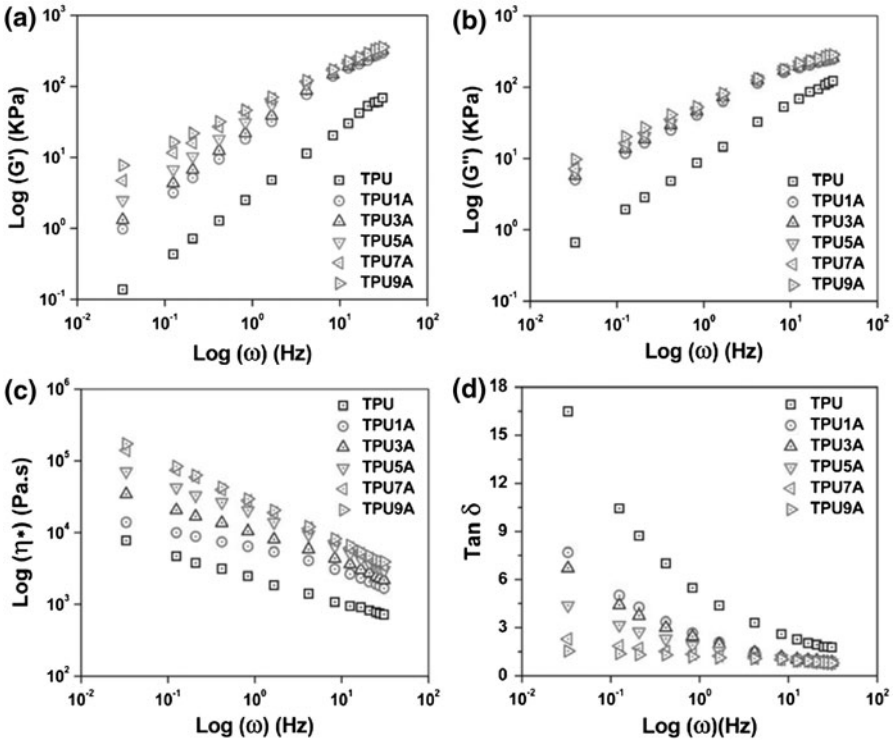

Fig. 4 Dynamic frequency sweep of **a** storage modulus (G'), **b** loss modulus (G''), and **c** complex viscosity (η^*), and **d** damping factor (tan δ) for neat TPU and its nanocomposites containing various wt% of OMMT loadings at a test strain of 0.98% and at a temperature of 145 °C

from liquid-like to solid-like behaviors occurs at a crossover frequency (ω_c) and 5 wt% Cloisite 15A can be regarded as rheological percolation limit. The magnitude of crossover frequencies of nanocomposites shift toward the lower frequency side with the increase in layered silicate content is called pseudo-solid-like behavior, which may occurs due to the slower molecular dynamic relaxation phenomenon.

It is observed from Fig. 4c that the η^* decreases with the increase in frequency. This is due to the strong shear thinning behavior of the polymer nanocomposites and their pristine equivalent at the melted condition. The substantial enhancement of η^* value of the nanocomposites with the increase in nanoclay content is attributed to the nanoscale dispersion of the Cloisite 15A in the TPU matrix, which improves the compatibility due to the strong interfacial interactions between organoclay and polymer matrix. This enhancement can be explained on the basis of resistance to flow and deformation of the molten polymer chains imposed by the tethered nanoclay particles along with the high aspect ratio and the shape of the silicate platelets, which favor the formation of structural networks even at very low silicate content. The dynamic viscosity at high frequency region is appreciably higher as compared to pristine TPU because the intercalated or exfoliated nanocomposites drag the movement of polymer chains in the molten condition.

The variation of ratio of the energy lost to the energy stored in a cyclic deformation, i.e., loss angle ($\tan \delta = G''/G'$) against dynamic angular frequency (ω) for neat TPU and various TPU nanocomposites to compare the liquid-like versus solid-like behavior of nanocomposites are shown in Fig. 4d. The virgin TPU shows maximum $\tan \delta$ value in the applied frequency range because external shear stress is homogeneously distributed throughout the polymeric system. The $\tan \delta$ value of the nanoclay-filled system is very low as compared to the pristine TPU at low frequency region because shear deformation leads to the partial orientation of the polymer chains, which indicates that Cloisite 15A enabled well-dispersed nanocomposites with solid-like behavior and higher reinforcing effect imparted by the more dimensionally stable layered silicates. The non-linear nature of $\tan \delta$ versus ω plot changes to a straight line with increase in nanoclay concentration in TPU matrix, which is due to the reduction in frequency dependence of G' at low frequency region. At lower filler loading (up to 5 wt%), the $\tan \delta$ value decreases with frequency but in case of higher filler loading (above 5 wt%) the $\tan \delta$ value is not significantly changed with applied frequency, which indicates that the incorporation of OMMT into TPU matrix improves the elastic properties of the matrix. However, the concentration of the three dimensional network is still very low, whereas the appearance of the arc in the plots of $\tan \delta$ versus ω shows evidence of the existence of a high order structure. The decrease in loss factor is more significant at low frequency region, whereas at high frequency region the decrease of $\tan \delta$ with increasing frequency is attributed to the partial orientation of TPU chains caused by shear deformation. The $\tan \delta$ of TPU nanocomposites gradually shifted to lower value with increasing nanoclay loading that imply the changes in the microstructures and the formation of regional network structures. Furthermore, at higher nanoclay loading the inter-particle network concentration is higher enough to restrict the mobility and deformability of the soft and hard segments of TPU chains leading to a characteristic modulus plateau.

The variation of shear modulus G' with applied angular frequency during filler–filler network structure formation at higher wt% nanofiller loading is studied by normalizing the modulus of the nanocomposites (G_c') with respect to that of the pristine TPU counterpart (G_p') at a lowest applied frequency of 0.033 Hz. The dependency of G_c'/G_p' ratio with nanoclay content (φ_i) is depicted in Fig. 5a. The value of G_c'/G_p' ratio increases gradually with an increase in φ_i. The G_c'/G_p' values are not significantly increased for lower nanoclay-loaded (1–3 wt%) TPU nanocomposites than that of the pristine TPU matrix. However, around 2-fold increase in G_c'/G_p' value is observed at 5 wt% of nanoclay loading. Furthermore, above 5 wt% nanoclay loading a rapid increase in the G_c'/G_p' value is experienced with increasing value of nanofiller weight fraction. Thus, it can be concluded that the dynamic rheological properties of the TPU/Cloisite 15A nanocomposites are strongly dominated by the TPU matrix at lower nanoclay loading, whereas a transition from liquid-like response to solid-like response is observed in TPU nanocomposites having nanoclay higher than 5 wt%. The solid-like viscoelastic behavior resulting from the formation of percolation network at around 5 wt% nanoclay content indicates the "dynamic rheological percolation

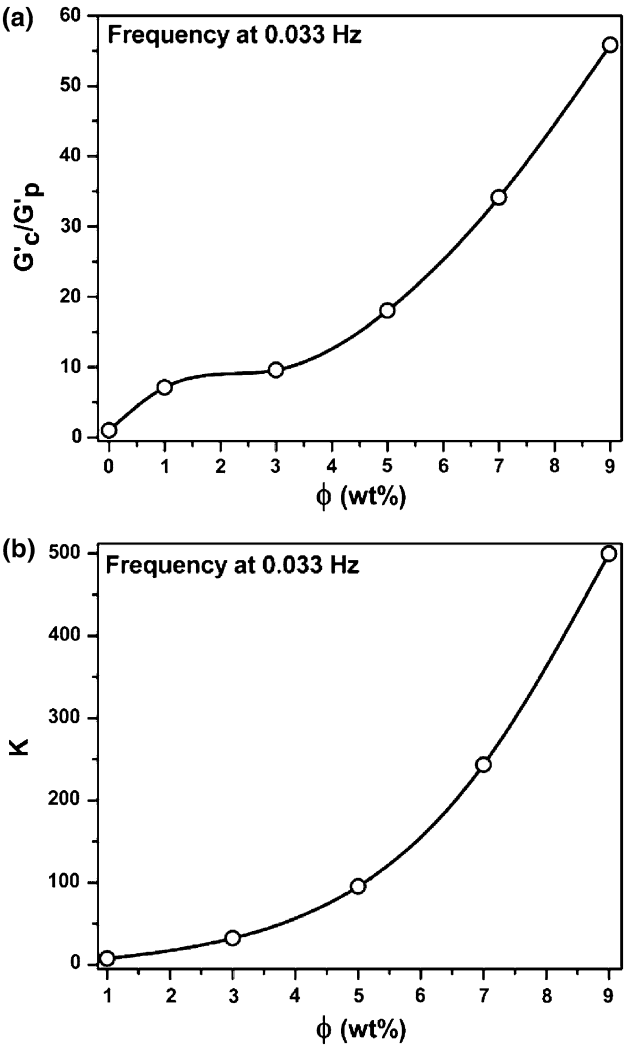

Fig. 5 Variation of **a** $G_c^{'}/G_p^{'}$ and **b** K with different wt% of Cloisite 15A nanoclay loading at frequency of 0.033 Hz for neat TPU and its nanocomposites

threshold" of TPU nanocomposites. WAXD and TEM results also confirmed that up to 5 wt% of nanoclay-loaded TPU nanocomposites have both mixed morphology of exfoliated and/or intercalated nanostructure, whereas beyond 5 wt% of nanoclay loading exfoliation starts to decrease that become predominantly intercalated and latter on formation of nanoclay agglomerates/tactoids.

The major theories describing the dependency of dynamic viscoelastic behavior on the filler weight fraction of the diluted and moderately filled polymeric systems are generally in accordance to the hydrodynamic approach coined by Albert Einstein [18]. The fundamental simple Kerner–Nielsen micromechanics model

proposed by Kerner [19] and further generalized by Nielsen [20] for the shear modulus of polymer composites is mentioned as below:

$$\frac{G_c^{'}}{G_p^{'}} = \frac{(1 + AB\varphi_i)}{(1 - B\psi\varphi_i)} \tag{1}$$

$$B = \left(\frac{G_f^{'}}{G_p^{'}} - 1\right) \Big/ \left(\frac{G_f^{'}}{G_p^{'}} + 1\right) \tag{2}$$

$$A = k_E - 1 = (7 - 5\nu_m/8 - 10\nu_m) \tag{3}$$

$$\psi = 1 + \left(\frac{1 - \varphi_m}{\varphi_m^2}\right)\varphi_i \tag{4}$$

where $G_c^{'}$, $G_p^{'}$, and $G_f^{'}$ are the dynamic shear storage modulus of the TPU nanocomposites, TPU matrix, and nanofiller, respectively. φ_i is the weight fraction of the nanofiller loading; and φ_m is the maximum packing fraction of the nanofiller ($\varphi_m = 0.637$ for randomly compact packing of highly rigid circular particles). ν_m is the Poisson's ratio of the polymer matrix and k_E is the Einstein's coefficient. ν_m and B are the factors that primarily related to the matrix–filler stiffness ratio. B is equal to unity ($B \approx 1$) for rigid and dimensionally stable nanoparticles ($G_f^{'} \gg G_p^{'}$). $\varphi_i\psi$ is the relative weight fraction. $\varphi_i\psi$ is equal to unity ($\varphi_i\psi \approx 1$) when $\varphi_i \approx \varphi_m$. The parameter "$A$" is reported to be sensitive to the amount of nanofiller aggregates, configurational geometry of the nanofillers, and Poisson's ratio (ν) of the TPU matrix. The Eq. 1 particularly represents the relative modulus ($G_c^{'}/G_p^{'}$) when φ_i is lower than the critical value (φ_c) ($\varphi_i < \varphi_c$), because above the critical concentration of nanofiller the silicate layers agglomerate to form filler–filler highly crosslinked network structures as a result the rheological properties of the filled TPU system changes from a viscous (liquid-like) to an elastic (solid-like) response. As suggested from Eq. 1, the number of aggregates and the geometry of the nanofiller remains the same and the coefficient A can be considered to be constant when φ_i value is very low, whereas when φ_i value is high the variation of particle agglomeration results in the variation of A. Therefore, it is necessary to modify the Kerner equation by the substitution of variable K for A. A useful modified generalized representation of the Kerner–Nielson equation is given as follows:

$$\frac{G_c^{'}}{G_p^{'}} = \frac{(1 + KB\varphi_i)}{(1 - B\psi\varphi_i)} \tag{4}$$

The variation of K with φ_i is represented in Fig. 5b. The value of K is calculated from Eq. 2 by considering the assumption that B is equal to unity and φ_m is equal to 0.637. When φ_i is less than 5 wt%, K value increases gradually. However, K increases rapid after 5 wt% of filler loading. Furthermore, the value of K is relevant to the number of particle aggregates and it increases with increase in filler–filler aggregates.

Figure 6a represents Han curves of G' versus G'' (the changes in low frequency region data is clearly shown in the inserted log G' versus log G'' plot) for the unfilled

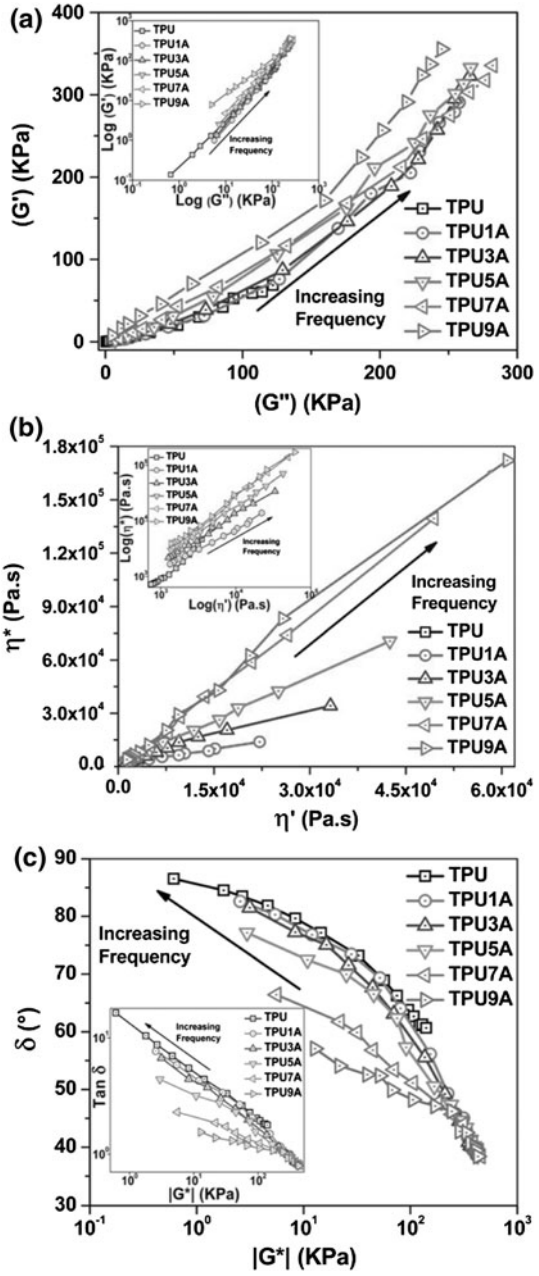

Fig. 6 **a** Han plot of storage modulus (G') versus loss modulus (G''), **b** Cole–Cole plots of imaginary viscosity (η^*) versus real viscosity (η'), and **c** van Gurp–Palmen plots of phase angle (δ) versus complex modulus ($|G^*|$) for neat TPU and its nanocomposites containing various wt% of OMMT loadings with frequency as a parameter

TPU and various wt% nanoclay filled TPU as a function of frequency at a fixed temperature. The structural differences between the TPU matrix phase and Cloisite 15A dispersed phase at a given temperature are generally investigated by the Han plot [21]. The neat TPU and TPU nanocomposites show nearly similar pattern of G'

versus G'' plot, which indicates same qualitative co-continuous structural system. The OMMT-based TPU nanocomposites exhibit some scattered data at lower frequency region (terminal zone) as shown in the inserted Fig. 6a, which is directed to the development of heterogeneous structures in the clay-filled systems. However, at higher frequency region (rubbery plateau) all the curves are super imposed to become a master curve, which is attributed to the appearance of homogeneous structure for different wt% clay loaded samples. The different behavior observed at lower and higher frequency is attributed to the difference in dynamic relaxation process for pristine TPU and nanocomposites. The applied shear stress at low frequency range is not sufficient enough to disintegrate the interconnected or crosslinked network-like structure that originating from the interactions between TPU chains and nanoclays as a result it becomes heterogeneous below a critical shear force. Furthermore, at higher frequency range the shearing force is well capable off to separate the three dimensional network structure of nanocomposites to form an isotropic and homogeneous state with the shearing force [22]. The G' versus G'' plot for clay-filled samples shifted to the higher modulus side is attributed to the increase in surface area as the amount of nanoclay is increased from 1 to 9 wt%, which arises due to the existence of interphase interactions between TPU matrix and nanoclay. The slope calculated from the curve corresponding to neat TPU matrix at molten state is assigned to be 2 and its value reduced for plots of above 5 wt% nanoclay-filled TPU nanocomposites, consequently curves deviated from the master curve corresponding to virgin TPU. This indicates that higher amount of clay-filled polymeric system become more heterogeneous as compared to the lower wt% filled samples. The change in the slope of the curve also concluded that the interphase interaction between matrix and nanofiller increases with inclusion of different wt% of nanoclay [23].

Figure 6b shows Cole–Cole plots of imaginary viscosity (η^*) versus real viscosity (η') for the neat TPU and its nanocomposite samples with frequency as a parameter (logarithmic plot of η^* versus η' in dynamic rheology is used to clearly represent the low viscosity data as shown in inserted plot). A Cole–Cole plot produces a master curve with a slope of 2 for isotropic and homogeneous polymer melts [24]. The amount of deviation from the slope of 2 is usually employed to find out the degree of heterogeneity developed in polymeric systems after addition of nanofillers. The TPU nanocomposites show a deviation from an arc-shaped pattern to a linear shape, i.e., provide a perfect single master curve, and exhibit shifting and changing of the slope of the plots with increasing wt% of nanoclay content, which implies that some conformational changes of nanostructures taken place with the inclusion of layered silicates. The change in the slope of the curves of η^* versus η' also indicates that the interphase interaction between TPU matrix and layered silicate increases obviously with the addition of nanoclay [25]. At a given η^* value, the η' value increases significantly with increase in nanoclay content. The plots for TPU/OMMT nanocomposites of different compositions do not fall on the single master curve that reveals the different nanostructures developed for different formulations. Cole–Cole plots are generally utilized for the representation of dynamic rheological properties and to explore the structural variation in heterogeneous polymeric materials with a dynamic relaxation time distribution at a constant temperature [26].

The substantial transformation from liquid-like (elastic behavior) to solid-like (viscoelastic behavior) is responsible for the rise of linear shape in the Cole–Cole plots for TPU/Cloisite 15A nanocomposites reinforced with 5 wt% nanoclay and more. The dynamic relaxation process is much longer with increasing nanoclay concentration in TPU matrix due to the formation of percolated filler–filler networks as a consequence the Cole–Cole plot geometry is affected significantly. The microstructure of nanocomposites drastically retard the long range molecular motion of the polymer chains of the filled systems and consequently results in large relaxation process by increasing the elasticity to viscosity ratio of TPU nanocomposites.

The Fig. 6c represents the plots of the phase angle ($\delta = \tan^{-1}(G''/G')$) versus the absolute value of the complex modulus ($|G^*| = (G'^2 + G''^2)^{1/2}$) for the neat TPU and TPU/Cloisite 15A nanocomposites measured at 145 °C with frequency as a parameter to determine the percolation threshold of the nanoclay content (the plots of tan δ versus $|G^*|$ are shown in inserted figure). This plot is known as the van Gurp–Palmen plot, which is accepted as a method to determine the "rheological percolation" of nanocomposites. The phase angle tends to 90° at low G^* value below the percolation threshold that consistent with a behavior dominated by the viscous flow. The phase angle significantly decreases with the modulus in agreement with an increasing elastic behavior at and beyond the percolation threshold. The phase angle prominently reduced and smaller δ values exhibited at lower complex modulus (G^*) region with increase in layered silicate content implies that the elastic characteristic of the TPU nanocomposites enhanced by the incorporation of organoclay. Determination of the rheological percolation thresholds of polymer–clay nanocomposites can be determined by enhancing the level of low frequency modulus or decrease the level of phase angle obtained from van Gurp–Palmen plot [27]. The curves for lower wt% nanofiller based TPU nanocomposites and their virgin counterparts approach towards linearity with 90° phase angle referring to the primary flow characteristic of a viscoelastic fluid/liquid. The significant decrease in phase angle with decreasing modulus shows the rise in elastic behavior of the TPU nanocomposites with incorporation of nanoclays. The viscoelastic transition from viscous fluid to elastic solid is observed after 5 wt% nanoclay content implying a rheological percolation threshold. This rheological percolation mainly arises because of the strong filler–filler layer interactions, which conclude that other physico-mechanical properties of the TPU nanocomposites is also experienced similar transitions to significant extent at around 5 wt% critical filler loading.

Temperature sweep test

The temperature dependency of the dynamic viscoelastic properties of TPU nanocomposites and their pristine counterpart in the solid and the melted state were obtained from the isochronal dynamic temperature sweep at 2.79% strain and 16.667 Hz angular frequency. Figure 7a shows the variation of G' as a function of applied temperature. The value of G' for virgin TPU initially decreases rather slowly with increase in temperature up to 75 °C and then gradually falls as the temperature is increased further and finally it becomes minimized. The significant drop of

modulus of the TPU is mainly attributed to the order–disorder transition (ODT) or microphase separation transition (MST) taking place at higher temperature range, which is defined as the temperature at which G' value begins to drop precipitously from isochronal dynamic temperature sweep experiment known as the MST temperature (T_{MST}) or ODT temperature (T_{ODT}) [28]. Figure 7a describes that the G' value of TPU nanocomposites initially decrease with temperature up to 130 °C followed by a rather slow reducing trend up to temperature of 190 °C with subsequent rapid decrease, whereas G' values of the Cloisite 15A-based TPU nanocomposites exhibit higher G' value throughout the scanned temperature range as compared to that of neat counterpart. The abrupt increase in dynamic storage shear modulus in the TPU nanocomposites than that of neat TPU at temperature above 130 °C is referred to the existence of some strong force of interaction among polymer and filler. It is also suggested that the TPU nanocomposites may possible undergo a first order transition from one ordered state to another, which is referred to the order–order transition (OOT) at about 130 °C and it remains intake over the entire range of temperature investigated up to 225 °C [29].

Figure 7b shows the variation of G'' with temperature for neat TPU and TPU/Cloisite 15A nanocomposites. It is observed that the value of G'' for pristine

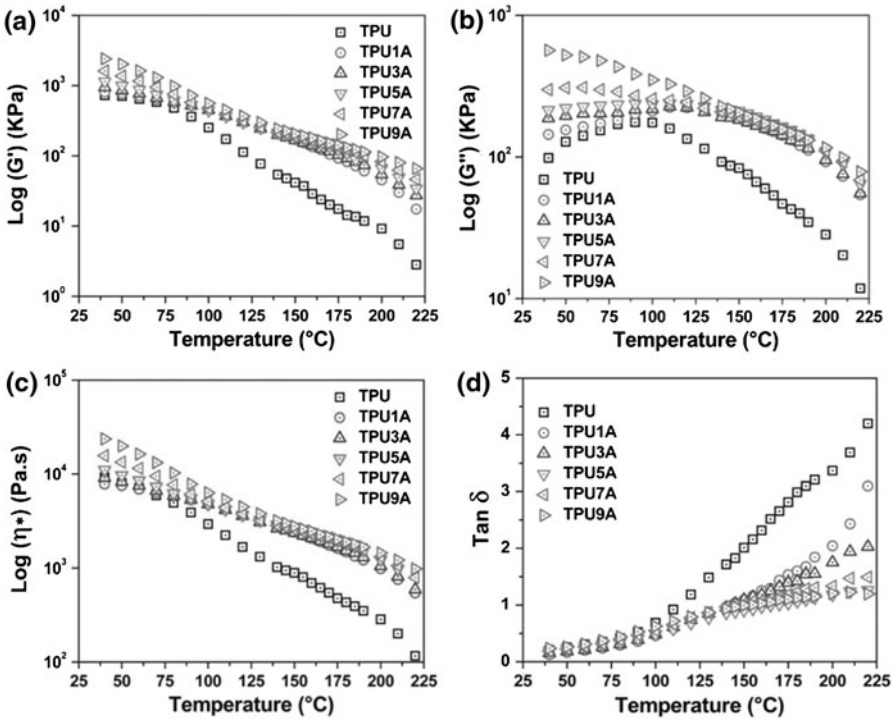

Fig. 7 Temperature sweep of **a** storage modulus (G'), **b** loss modulus (G''), **c** complex viscosity (η^*), and **d** damping factor (tan δ) for neat TPU and its nanocomposites containing various wt% of OMMT loadings at a test strain of 2.79% and at a frequency of 16.667 Hz

counterpart shows an initial rise up to 60 °C after that it rapidly decreases with increase in temperature due to the dynamic molecular relaxation of soft and hard segment domains in TPU matrix. The value of G'' for the TPU/Cloisite 15A nanocomposites containing up to 5 wt% nanoclay loading first increases slowly with increase in temperature up to 110 °C then falls drastically with a further increase in temperature. The prominent broad transition peak detected in the plot is because of the phase transition taken place between soft TPU matrix phase and rigid layered silicate dispersed phase, which resulted from the restricted dynamic relaxation characteristics. At lower temperature range up to 110 °C, G'' value decreases rapidly with increase in temperature above 5 wt% nanoclay loaded TPU nanocomposites, which is mainly attributed to the highly crosslinked structures of the filler–filler agglomerates.

Figure 7c shows the effect of temperature on η^* for neat TPU and its nanocomposites. It has been observed that the values of η^* for TPU nanocomposites increase with increase in nanoclay content and decrease steadily with increase in temperature throughout the investigated temperature range. Furthermore, the significant reduction of viscosity beyond 130 °C in nanoclay-filled TPU matrix, which is mainly confined to the development of highly network structures at the time of physical crosslinking at higher temperature region. The hindrance faced during flow of polymer melts become less experienced and flow units become highly energized with increase in temperature because of the increase in free volume of the polymeric system in molten state at higher temperature, consequently the relaxation time and melt viscosity is reduced substantially.

Figure 7d represents the effect of temperature on the loss tangent of neat TPU and its nanocomposites. Tan δ increases uniformly throughout the scanned temperature range for all the polymeric systems. At lower temperature region, the damping behavior is not affected significantly with temperature because of the solid-like behavior ($G' > G''$) of materials. However, at higher temperature region a significant difference of loss tangent is marked among TPU nanocomposites and their counterpart due to the beginning of softening of the TPU matrix at around 130 °C as a consequence the viscous component of dynamic shear modulus control the melt rheology of polymeric system rather than the elastic component ($G' < G''$) of modulus. The flow ability of the polymer melt is restricted and the viscosity effect is compensated by the dimensionally more stable and rigid nanoclay particles at temperature above 130 °C as a result a plateau region in the tan δ curves is found for the nanoclay reinforced TPU matrix. The tan δ curve shifts towards the lower value site with addition of organoclay that refers to the improvement of elastic behavior of the TPU matrix. The tan δ value is the ratio of G'' upon G' and a reduction in this ratio with wt% nanoclay loading indicates that the TPU nanocomposites has a higher G' or elastic characteristic is improved substantially as compared to the pristine counterpart. The polymer–filler network structures formed in the layered silicate-filled TPU system leading towards the lower plastic deformation.

Stress relaxation behavior

Figure 8 shows the RPA stress relaxation curves for neat TPU and TPU nanocomposites with different wt% of nanoclay contents. The slopes of modulus

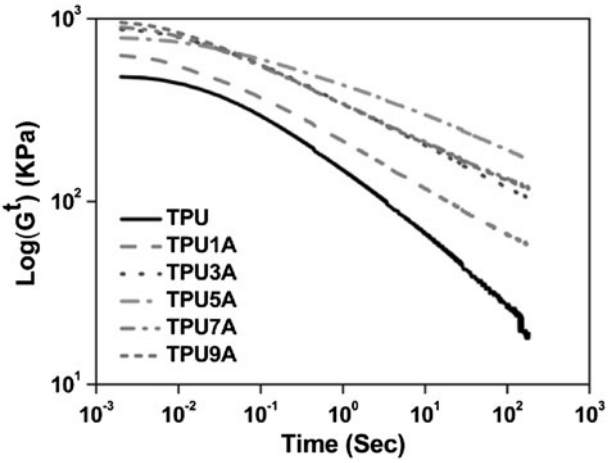

Fig. 8 RPA stress relaxation plots for neat TPU and its nanocomposites containing various wt% of OMMT loadings

(G^t) curves decrease with the increase in nanoclay content, which indicates that the relaxation time increases with the increase in wt% of nanoclay loading as a result the dynamic relaxation rate of nanocomposites are substantially slower than that of pure TPU. The plateau zone is evident for the neat TPU matrix and TPU/OMMT nanocomposites because more time is required to disintegrate the polymer entanglement networks. At plateau region, the stress value is strongly influenced by the organoclay content due to the contribution of nanoclay for strengthening the initial network structure. On the other hand, for virgin TPU the plateau zone is prominent, whereas for TPU nanocomposites the rubbery plateau is partly diminished because the viscosity of the TPU nanocomposites are higher than the viscosity of their unfilled counterpart, consequently the stress relaxation decay in the terminal zone is much faster for the TPU matrix when compared to those of the TPU nanocomposites. With increase in time the polymer back bone chains start to disentangle, hence longer polymer molecular chains require longer time for disentangle. As more and more chains relax, the concentration of unrelaxed chain becomes less and it promotes a further drop in modulus (G^t), which results a terminal modulus zone [30]. The modulus of TPU matrix is drastically failed throughout the stress relaxation decay process. The decay in the stress is more pronounced in case of unfilled system as compared to the filled one. The stress relaxation in the neat TPU is attributed to chain motion and orientations, rearrangement of broken chains, crosslinks, and entanglements, whereas filler structure and the interaction between filler and polymer are responsible for stress relaxation in filled system [31]. It is interesting to note that the characteristic relaxation time related to uncoiling/disentangling of soft segment chain network in the soft phase increases with the addition of clay that enhances the degree of microphase separation; which means that the hard segment content in the soft phase decreases, soft chain flexibility increases, and elasticity increases, hence leading to a

Table 2 Stress relaxation data of pure TPU and TPU/Cloisite 15A nanocomposites

Sample codes	Initial stress (σ_0) (KPa)	Equilibrium stress (σ_e) (KPa)	Relaxation ratio [{($\sigma_0 - \sigma_e$)/σ_0} × 100]	Relaxation rate index ($n \times 100$)
TPU	488.03	19.00	96.10	2.60
TPU1A	648.67	57.352	91.16	4.94
TPU3A	894.64	104.85	88.28	5.20
TPU5A	791.93	169.38	78.61	5.01
TPU7A	918.28	119.74	86.96	5.29
TPU9A	981.17	117.44	88.03	5.44

slow stress relaxation process. It is noted that the trend in the change of microphase separation with clay contents is consistent with the trend in the relaxation time.

The initial stress, equilibrium stress, and relaxation ratio are listed in Table 2. With the increase in clay content, both the initial stress and equilibrium stress increased. The addition of OMMT can improve the modulus of TPU matrix. The results indicate that the addition of organoclay has a very strong effect on the crosslink density of TPU. The relaxation ratio decreases with the addition of organoclay. There is a significant difference in the relaxation ratios between neat TPU and TPU nanocomposites. The increase in nanoclay content results in a decrease in the relaxation ratio, which is due to the presence of soft domains in the TPU matrix and also the increase in the amount of elastic crosslinked network structures [32].

Conclusion

The morphological studies of TPU nanocomposites revealed that Cloisite 15A organoclay was uniformly dispersed in the TPU matrix in a nanometer scale at lower nanoclay loading, whereas the random aggregation was observed above 5 wt% loading of nanoclay. Strain sweep study indicated that the TPU nanocomposites display a dynamic strain sensitive "linear viscoelastic behavior" region much narrower than that of the neat TPU matrix. The linear rheological material function showed that the nanocomposites are characterized by a solid-like behavior, which is revealed by the presence of a low frequency plateau region in storage modulus versus frequency plot. The domain of such plateau or pseudo-plasticity is found to be strongly dependent on the level of interfacial interactions between the TPU matrix and the surfactant of the modified layered silicates. Such specific interactions favor the degree of dispersion/distribution of the layered silicate platelets within the TPU matrix leading to formation of a "rheological percolation network". Beyond 5 wt% nanoclay loading the formation of percolation network taken place, which leads to enhancement of the low frequency normalized modulus. The strong shear shinning behavior of the TPU/OMMT nanocomposites resulted from the orientation of rigid molecular chains in the TPU nanocomposites. The storage modulus, loss modulus, and dynamic viscosity of TPUCN showed a

monotonic increase with OMMT content as observed from frequency sweep. The increase in the slope of the plot of log G' versus log G'' for the TPU nanocomposites with increase in OMMT content suggested that the microstructures of the nanocomposites were worst affected by the addition of nanoclay. The TPU/Cloisite 15A nanocomposites exhibited a smaller value of phase angle at lower complex modulus with increase in OMMT content, which implies that the elastic behavior of the nanocomposites are enhanced by the incorporation of nanoclay. It is observed that the plot between the complex viscosity against imaginary viscosity is significantly shifted towards upward direction at higher viscosity region, which may be due to the microstructural changes occurred in TPU matrix after inclusion of layered silicates.

Acknowledgments The authors would like to thankfully acknowledge the financial assistance supported by the Extra Mural Research Division II (EMR-II), Human Resource Development Group (HRDG), Council of Scientific and Industrial Research (CSIR), New Delhi 110012, India vide sanction no. 22(0410)/06/EMR-II dated 13-09-2006. The authors would like to thank Mr. S. Mustak for his assistance for conducting RPA test. The authors thank Miku Traders, Vadodara, Gujarat 390005, India, for providing Tecoflex® TPU for the research work.

References

1. Finnigan B, Martin D, Halley P, Truss R, Campbell K (2004) Morphology and properties of thermoplastic polyurethane nanocomposites incorporating hydrophilic layered silicates. Polymer 45(7):2249–2260. doi:10.1016/j.polymer.2004.01.049
2. Chen TK, Tien YI, Wei KH (2000) Synthesis and characterization of novel segmented polyurethane/clay nanocomposites. Polymer 41(4):1345–1353. doi:10.1016/S0032-3861(99)00280-3
3. Chang JH, An YU (2002) Nanocomposites of polyurethane with various organoclays: thermomechanical properties, morphology, and gas permeability. J Polym Sci B 40(7):670–677. doi:10.1002/polb.10124
4. Berta M, Lindsay C, Pans G, Camino G (2006) Effect of chemical structure on combustion and thermal behavior of polyurethane elastomer layered silicate nanocomposites. Polym Degrad Stab 91(5):1179–1191. doi:10.1016/j.polymdegradstab.2005.05.027
5. Vaia RA, Giannelis EP (1997) Lattice model of polymer melt intercalation in organically-modified layered silicates. Macromolecules 30(25):7990–7999. doi:10.1021/ma9514333
6. Ma X, Lu H, Liang G, Yan H (2004) Rectorite/thermoplastic polyurethane nanocomposites: preparation, characterization, and properties. J Appl Polym Sci 93(2):608–614. doi:10.1002/app.20423
7. Finnigan B, Jack K, Campbell K, Peter Halley P, Truss R, Casey P, Cookson D, King S, Martin D (2005) Segmented polyurethane nanocomposites: impact of controlled particle size nanofillers on the morphological response to uniaxial deformation. Macromolecules 38(17):7386–7396. doi:10.1021/ma0508911
8. Chavarria F, Paul DR (2006) Morphology and properties of thermoplastic polyurethane nanocomposites: effect of organoclay structure. Polymer 47(22):7760–7773. doi:10.1016/j.polymer.2006.08.067
9. Dan CH, Lee MH, Kim YD, Min BH, Kim JH (2006) Effect of clay modifiers on the morphology and physical properties of thermoplastic polyurethane/clay nanocomposites. Polymer 47(19):6718–6730. doi:10.1016/j.polymer.2006.07.052
10. Chun BC, Cho TK, Chong MH, Chung YC, Chen J, Martin D, Cieslinski RC (2007) Mechanical properties of polyurethane/montmorillonite nanocomposite prepared by melt mixing. J Appl Polym Sci 106(1):712–721. doi:10.1002/app.26721
11. Ran Q, Zou H, Wu S, Shen J (2008) Study on thermoplastic polyurethane/montmorillonite nanocomposites. Polym Compos 29(2):119–124. doi:10.1002/pc.20327

12. Meng X, Du X, Wang Z, Bi W, Tang T (2008) The investigation of exfoliation process of organic modified montmorillonite in thermoplastic polyurethane with different molecular weights. Compos Sci Technol 68(7–8):1815–1821. doi:10.1016/j.compscitech.2008.01.012
13. Barick AK, Tripathy DK (2010) Thermal and dynamic mechanical characterization of thermoplastic polyurethane/organoclay nanocomposites prepared by melt compounding. Mater Sci Eng A 527(3):812–823. doi:10.1016/j.msea.2009.10.063
14. Barick AK, Tripathy DK (2010) Effect of organoclay on the morphology, mechanical, thermal, and rheological properties of organophilic montmorillonite nanoclay based thermoplastic polyurethane nanocomposites prepared by melt blending. Polym Eng Sci 50(3):484–498. doi:10.1002/pen.21556
15. Payne AR (1962) The dynamic properties of carbon black-loaded natural rubber vulcanizates. Part I. J Appl Polym Sci 6(19):57–63. doi:10.1002/app.1962.070061906
16. Berta M, Saiani A, Lindsay C, Gunaratne R (2009) Effect of clay dispersion on the rheological properties and flammability of polyurethane–clay nanocomposite elastomers. J Appl Polym Sci 112(5):2847–2853. doi:10.1002/app.29771
17. Li J, Zhou C, Wang G, Zhao D (2003) Study on rheological behavior of polypropylene/clay nanocomposites. J Appl Polym Sci 89(13):3609–3617. doi:10.1002/app.12643
18. Einstein A (1950) On the motion required by the molecular kinetic theory of heat of small particles suspended in a stationary liquid. Ann Physik 17(8):549–560
19. Kerner EH (1956) The elastic and thermo-elastic properties of composite media. Proc Phys Soc Sect B 69(8):808–813. doi:10.1088/0370-1301/69/8/305
20. Nielsen LE (1970) Generalized equation for the elastic moduli of composite materials. J Appl Phys 41(11):4626–4627. doi:10.1063/1.1658506
21. Han CD, Jhon MS (2003) Correlations of the first normal stress difference with shear stress and of the storage modulus with loss modulus for homopolymers. J Appl Polym Sci 32(3):3809–3840. doi:10.1002/app.1986.070320302
22. Han SI, Lim JS, Kim DK, Kim MN, Im SS (2008) In situ polymerized poly(butylene succinate)/silica nanocomposites: physical properties and biodegradation. Polym Degrad Stab 93(5):889–895. doi:10.1016/j.polymdegradstab.2008.02.007
23. Liu Q, Chen D (2008) Viscoelastic behaviors of poly(ε-caprolactone)/attapulgite nanocomposites. Eur Polym J 44(7):2046–2050. doi:10.1016/j.eurpolymj.2008.04.035
24. Ottenbrite RM, Utracki LA, Inoue S (1987) Current topics in polymer science. Hanser, Munich
25. Han CD, Lem KW (1983) Temperature-independent correlation of elastic responses of viscoelastic liquids. Polym Eng Rev 2(1):135–165
26. Cole KS, Cole RH (1941) Dispersion and absorption in dielectrics I. Alternating current characteristics. J Chem Phys 9(4):341–351. doi:10.1063/1.1750906
27. Van Gurp M, Palmen J (1998) Time-temperature superposition for polymer blends. Rheol Bull 67(1):5–8
28. Yoon PJ, Han CD (2000) Effect of thermal history on the rheological behavior of thermoplastic polyurethanes. Macromolecules 33(6):2171–2183. doi:10.1021/ma991741r
29. Choi S, Lee KM, Han CD (2004) Effects of triblock copolymer architecture and the degree of functionalization on the organoclay dispersion and rheology of nanocomposites. Macromolecules 37(20):7649–7662. doi:10.1021/ma030585s
30. Dick JS, Pawlowski H (1997) Application for stress relaxation from the rubber process analyzer in characterization and quality control. Rubber World 215(4):21–30
31. Xia H, Shaw SJ, Song M (2005) Relationship between mechanical properties and exfoliation degree of clay in polyurethane nanocomposites. Polym Int 54(10):1392–1400. doi:10.1002/pi.1858
32. Xia H, Song M, Zhang Z, Richardson M (2007) Microphase separation, stress relaxation, and creep behavior of polyurethane nanocomposites. J Appl Polym Sci 103(5):2992–3002. doi:10.1002/app.25462